Available online at www.sciencedirect.com
SCIENCE DIRECT®
International Journal of Coal Geology 57 (2004) 99–116
International Journal of COAL GEOLOGY
www.elsevier.com/locate/ijcoalgeo

Graphite, semi-graphite, natural coke, and natural char classification—ICCP system

B. Kwiecińska[a], H.I. Petersen[b,*]

[a] *Faculty of Geology, Geophysics and Environmental Protection, AGH University of Science and Technology, Al. Mickiewicza 30, 30-059 Cracow, Poland*

[b] *Geological Survey of Denmark and Greenland (GEUS), Øster Voldgade 10, DK-1350 Copenhagen K, Denmark*

Received 18 August 2003; received in revised form 19 September 2003; accepted 23 September 2003

Abstract

This document presents the International Committee for Coal and Organic Petrology (ICCP) classification of four organic components that cannot be included into any of the three maceral groups vitrinite, inertinite and liptinite: (1) Graphite; (2) Semi-graphite; (3) Natural coke; and (4) Natural char. Graphite and semi-graphite are related to high metamorphic grades and can be considered as end-members of the continuous coalification process of organic matter initially deposited as peat. Natural coke is formed from coal by a relatively local elevated heat flow caused by an intrusive body and it may thus occur in a range of coalification stages. Influence of heat from fire on coal or on gelified organic matter in peat forms natural char which therefore also occurs in a wide range of coalification stages.

Keywords: Graphite; Semi-graphite; Natural coke; Natural char; Classification; ICCP

1. Introduction

The International Committee for Coal and Organic Petrology (ICCP) is continuing to revise ICCP's classification systems for macerals as seen in reflected light. A new vitrinite classification system was published in 1998 (ICCP, 1998) and in 2001, the new inertinite classification system was likewise published (ICCP, 2001). Both these final systems, collectively referred to as the "ICCP System 1994", are the result of the work of two editorial groups, combined with extensive discussions and revisions of prepared drafts during several annual ICCP meetings attended by numerous international experts.

This document presents the ICCP classification of graphite, semi-graphite, natural coke, and natural char. The definitions of these four components have been presented, discussed, and approved at annual ICCP meetings just as the macerals of the "ICCP System 1994" were. Graphite, semi-graphite, natural coke, and natural char do not fit any maceral definition of the three maceral groups (vitrinite, inertinite and liptinite) and are therefore treated together in this document. Graphite and semi-graphite are principally formed by graphitization and, essentially, they are end-member products of the continuous transformation of organic matter (coalification) from peat through bituminous coals and anthracite to graphite.

* Corresponding author.
E-mail address: hip@geus.dk (H.I. Petersen).

0166-5162/$ - see front matter © 2004 Elsevier B.V. All rights reserved.
doi:10.1016/j.coal.2003.09.003

They, therefore, represent a high metamorphic grade. In contrast, natural coke is derived from local elevated heat flow related to an intrusive body, and can thus be found in a range of coalification stages. Similarly, natural char occurs in a range of coalification stages as it is formed by the influence of heat from fire on coal or on gelified organic matter in peat.

2. Graphite

2.1. Origin of term

The term graphite was introduced by Werner (1789).

2.2. Definition

Graphite is a crystalline, polymorphic form of elementary carbon.

Comment. In isolated carbon atoms, the distribution of electrons is $1s^2\ 2s^2\ 2p^2$. Each carbon atom in the graphite crystal is hybridised trigonally, forming three σ and one π bonds. The hybridised orbitals of the sp^2 type give σ bonds of a length of 1.42 Å, arranged at 120° angles with respect to one another, with sheets made up of regular hexagons. The fourth electron of each atom, being in the p orbital, forms π bonds with all the neighbouring atoms.

Graphite has a heterodesmic layered structure. The structure of graphite consists of six-membered rings in which each carbon atom has three near neighbours at the apices of an equilateral triangle. Within the large planar layers, there are linkages intermediate between atomic and metallic bonds. The layers in the crystal are held together by van der Waals bonding forces of energy of 0.2 eV/atom. Perfect basal cleavage readily takes place between the layers along the (001) plane. Weak bonding perpendicular to the layers gives rise to easy gliding parallel to the sheets.

The model of graphitic structure proposed by Hull (1917) and described by Bernal (1924) assumes the existence of the basal, hexagonal crystalline lattice of the A 9 type. The unit cell in the hexagonal lattice of graphite contains four atoms with coordinates (000), (00(1/2)), ((2/3)(1/3)0) and ((1/2)(2/3)(1/2)) Space group D_{6h}^4-$P6_3/mmc$; unit cell dimensions: $a_0 = 2.46$ Å, $c_0 = 6.70$ Å, c/a ratio = 2.75; interlayer distance ($c/2$) = 3.3539 + 0.0001 Å.

Two types of spatial arrangement of carbon layers are possible: the sequence ABABAB... is characteristic of the hexagonal structure of graphite (Fig. 1A) while the sequence ABCABC... occurs in the rhombohedral modification (Fig. 1B).

In the sequence ABABAB..., the stacking of the layer planes is the following: every other carbon atom lies over the centre of a hexagon consisting of carbon atoms of the preceding layer, i.e. every other layer is translationally identical with respect to the *c*-axis. The hexagonal form of graphite is thermodynamically

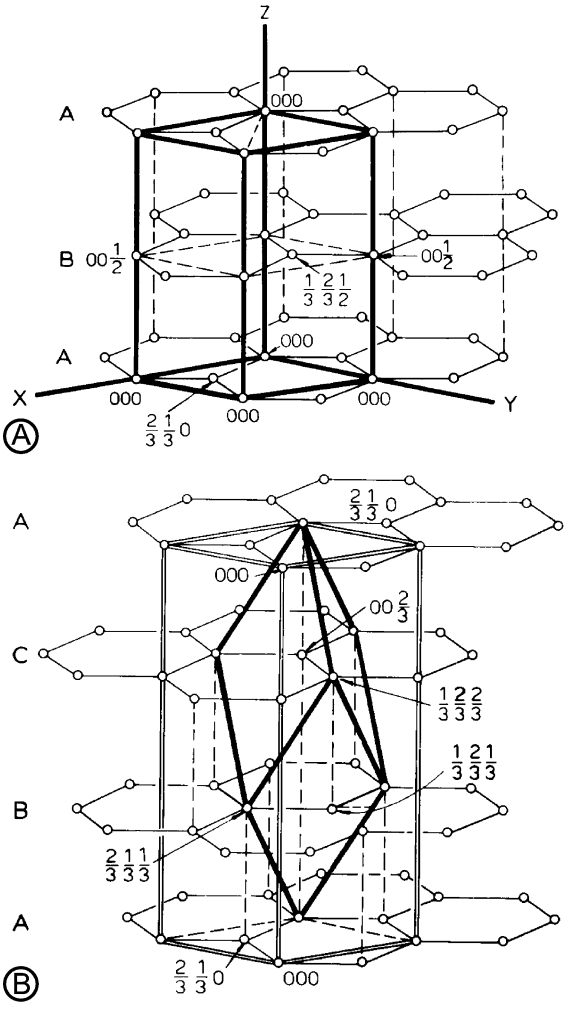

Fig. 1. (A) Hexagonal lattice of graphite (Reynolds, 1968); (B) Rhombohedral lattice of graphite (Reynolds, 1968).

stable over a range of temperatures and pressures ($T < \sim 2000$ °C, $P < 1.3 \times 10^{10}$ Pa [130 kbar]).

The rhombohedral modification is a metastable phase, disappearing at elevated temperatures (T>2000 °C). In this modification, every third layer is translationally identical, according to the sequence ABC-ABC…. This form has not been observed as a separate phase in the structure of natural graphite (Ubbelohde and Lewis, 1960; Reynolds, 1968). The rhombohedral phase has the space group D_{3d}^{5}-R3m with the atoms occupying the positions: (000), ((2/3)(1/3)0), (00(2/3)), ((2/3)(1/3)(1/3)), ((1/3)(2/3)(1/3)) and ((1/3)(2/3)(2/3)) Taking the hexagonal lattice as a basis, the unit cell parameters are: $a_0 = 2.46$ Å, $c_0 = 10.038$ Å.

The described structure of graphite refers to its crystalline forms defined as ideal models. However, in nature graphite usually appears in less perfect forms (real crystals) and in a variety of disordered types. As transitional phases, these forms show varying degrees of graphitization of carbon contained in the carbonaceous substance or organic matter dispersed in sedimentary or metamorphic rocks. They are called semi-graphite, meta-anthracite, and anthracite, according to the content of C and H and the degree of ordering of the lattice structure. For establishing transitional phases and pure graphite by the degree of their crystalline perfection, it is necessary to include maximum reflectance measurements (%R_{max}) (Table 1), X-ray investigations (Fig. 2), and transmission electron microscopy (TEM) (Figs. 3–7). In X-ray and electron diffraction, graphite is detected by the occurrence of sharp hkl reflections such as (101), (110), (112) and (114) which are evidence for three-dimensional crystalline order (McCartney and Ergun, 1965; Kwiecińska, 1980) (Figs. 2 and 7). Additional information can be obtained from scanning electron microscopy (SEM) (Figs. 8 and 9), Fourier-transform infrared spectroscopy (FTIR), differential thermal analysis (DTA), Raman microspectroscopy (Pasteris and Wopenka, 1991; Wopenka and Pasteris, 1993), and also from chemical and physical analysis. Usually the division into pure graphite and transitional forms is based on X-ray analysis, measurements of %R_{max}, and the H/C atomic ratio (Table 1).

Table 1
Graphite and transitional phases[a]

Varieties, phases	Symbol	d 002 (Å)	%Rmax	H/C
Graphite	G	3.354–3.37	>9.0	0.005–0.10
Semi-graphite	SG	3.37–3.38	6.5–9.0	0.10–0.15
Meta-anthracite	MA	3.38–3.40	<6.5	0.15–0.20
Anthracite	A	>3.40	<5.0	≥0.20

[a] Graphites occurring in different stress and temperature regimes may have different properties.

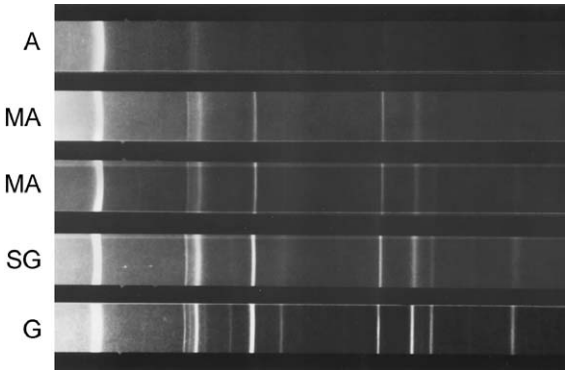

Fig. 2. X-ray powder photographs of graphitic substances. A: anthracite; MA: meta-anthracite; SG: semi-graphite; G: graphite; d_{hkl} from the left to the right: (002), (100), (102/3), (101), (104/3), (102), (004), (108/3), (103), (110), (112), (006), (106), (114).

2.3. Occurrence

Graphite occurs in different forms in various types of rocks and deposits:

1. dispersed cryptocrystalline pigment and cryptocrystalline dust concentrated in microlaminae,

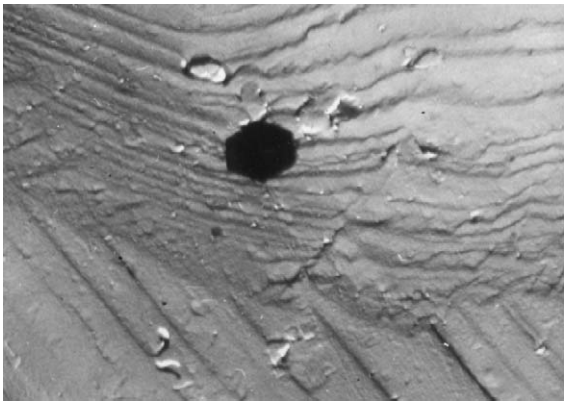

Fig. 3. Hexagonal graphite crystallite on fracture-surface of marble. Przeworno, Lower Silesia, Poland. Transmission electron microscopy.

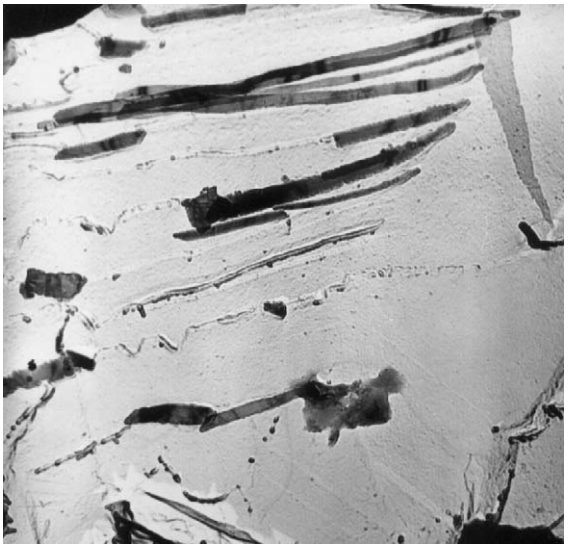

Fig. 4. Partly split graphite laths, extracted from fracture-surface of marble. Przeworno, Lower Silesia, Poland. Transmission electron microscopy.

schlieren, streaks, and bands in phyllites, quartzites, crystalline slates, and fine-grained marbles;
2. submicroscopic crystallites aggregated in scaly-granular forms in quartzite schists and quartzites;
3. xenoblastic microfragments in meta-conglomerates;
4. distinct crystaloblasts, single flakes, scales, plates or lamellae, disseminated flakes in gneisses, pyroxene granulites and coarse-grained marble (Figs. 3–6, 8 and 10);
5. impregnations in the form of pyrolitic nodules or rosette forms in igneous rocks (Figs. 9 and 11);
6. irregular patches enclosed within tonalites;
7. lumps, pieces, fragments, and monocrystalline flakes in seams, lenses, veins, fissures, and nests in granulites and other deposits;
8. pseudomorphs;
9. spherical aggregates resulting from polycentric growth occurring in anorthosites (Kvasnitsa et al., 1999).

Typical mineral associations are: goethite, hydrohematite, ilmenite, anatase, and bruckite.

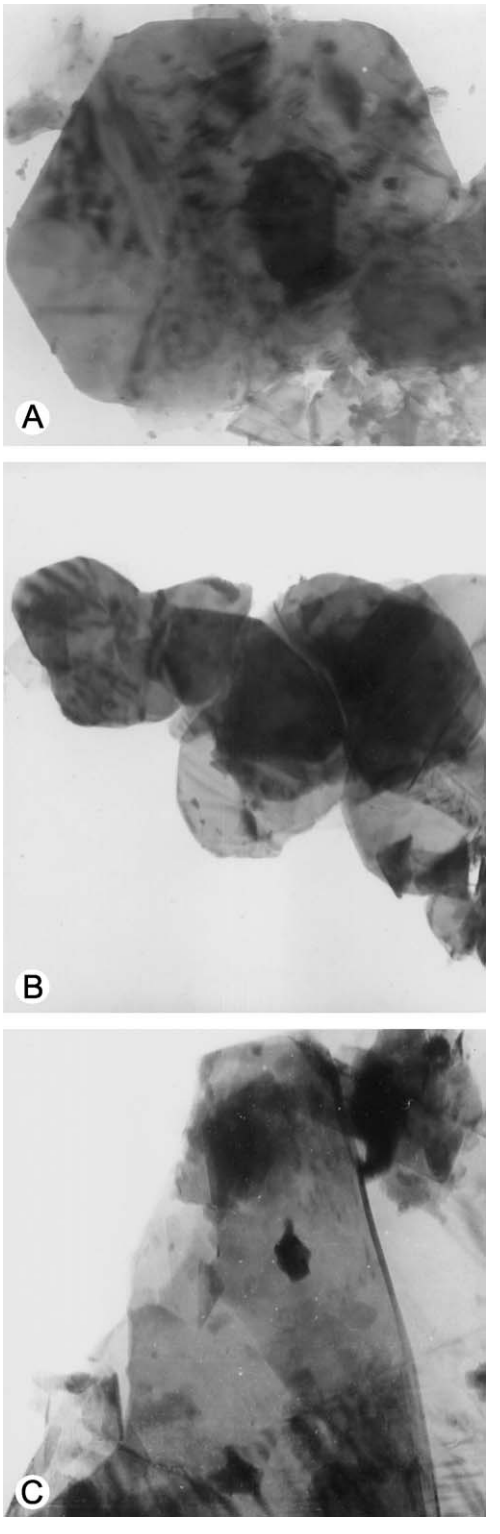

Fig. 5. (A) Graphite flake with hexagonal habit. Borrowdale, England; (B) Aggregated graphite flakes with rounded outlines. Borrowdale, England; (C) Graphite flakes. Male Vrbno, Czech Republic. All transmission electron microscopy.

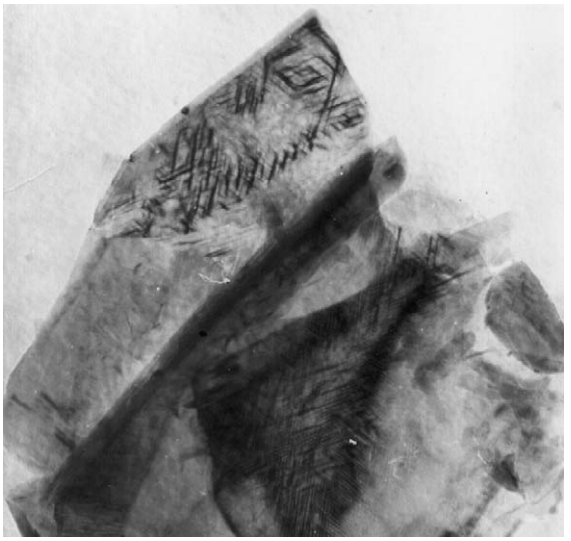

Fig. 6. Rhombic Moire effect resembling growth spirals. Male Vrbno, Czech Republic. Transmission electron microscopy.

Typical graphitic parageneses consist of pyrite, pyrrhotite, magnetite, siderite, and calcite.

2.4. Physical properties

Properties and morphology of graphite reflect its highly anisotropic structure. Graphite crystals exhibit extreme softness and flexibility.

2.4.1. Macroscopic observations

The first measurements of the graphite crystals, by the goniometric method, were made by Palache (1941). This is a unique and important contribution to the descriptive mineralogy of graphite. The natural crystals from Sterling Hill New Jersey, described and drawn by Palache, are a recognized standard for well-formed graphite crystals and they are still considered to be some of the highest quality crystals reported in the literature (Jaszczak, 1994).

Graphite assumes different morphological forms. It can be flat, fibrous, and spherical. Graphite crystals can be divided into several groups depending on the colour, lustre, cleavage, size, habit, and also the mode of occurrence (Kwiecińska, 1980). Large crystals exhibit a habit of hexagonal flakes, plates, or scales. They are silvery in colour, with strong metallic lustre and perfect basal cleavage. Single crystals are up to several mm in size, whereas macrocrystalline concentrations range from 5 to 100 mm. In microcrystalline aggregates from 1.0 to 0.1 mm in size, graphite flakes are frequently rounded on the edges. Microcrystalline forms of graphite show a semi-metallic lustre. Cryptocrystalline graphite of a crystal diameter less than 100 μm forms granular and fibrous aggregates blackish-grey and black in colour. Aggregated forms display greasy, silky or earthy (dull) lustre.

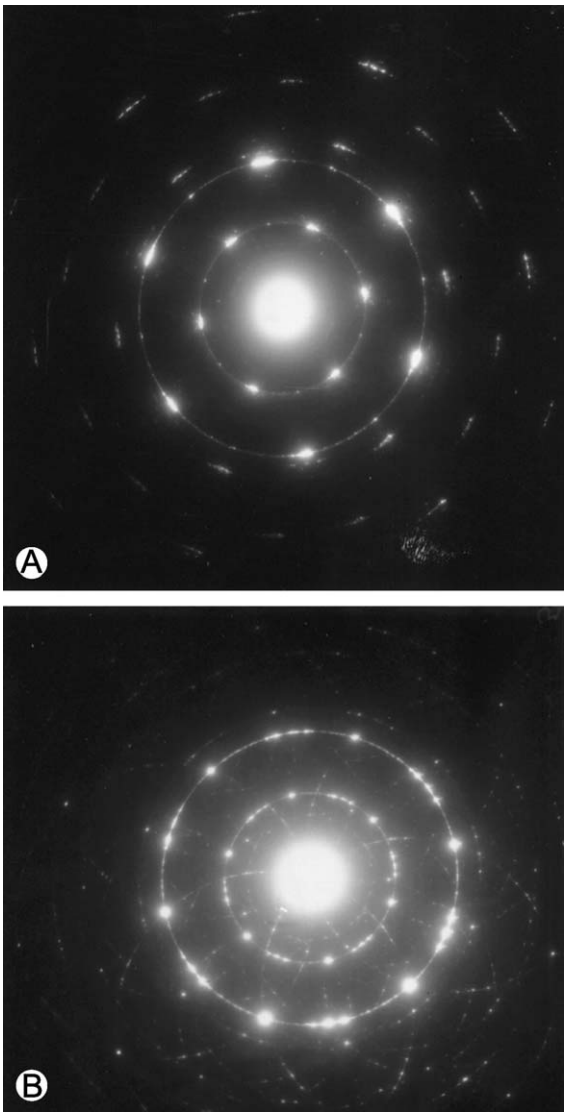

Fig. 7. (A) Electron diffraction pattern of graphite monocrystal. Ticonderoga, USA; (B) Electron diffraction pattern of graphite with distinct texture. Rodope, Bulgaria. Both transmission electron microscopy.

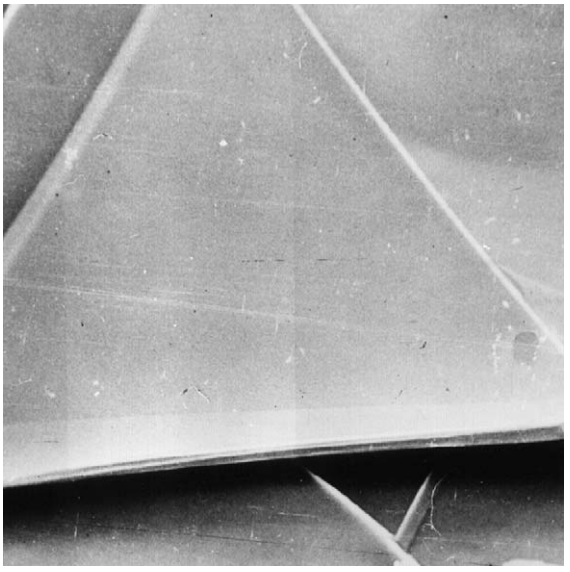

Fig. 8. Surface of graphite crystals (// 001), Sri Lanka. Scanning electron microscopy.

2.4.2. Microscopic features

Different forms of microscopic features appear in respective rock types. Cryptocrystalline graphite appears in the form of pigment colouring rocks (recrystalline limestones, marbles, phyllites, slates).

Fig. 9. Spheroidal surface type (rosette structure). Borrowdale, England. Scanning electron microscopy.

Cryptocrystalline graphitic dust also forms microlaminae, schlieren, and streaks; sometimes with visible microfolds showing flexural texture. In quartzitic schists and quartzites, graphite has a scaly-granular form or exhibits aggregated forms of concentration. Crystalloblasts and scales can be seen, markedly ragged, "hook-like" and irregular in outline. In addition, tablets, hexagonal flakes (Figs. 3 and 5A), and plates are visible. In metamorphic rocks of a higher grade of metamorphism (amphibolite and granulite facies), graphite shows a distinct crystalline form as isolated idioblasts and as lath-like (Fig. 10), fibrous, platy, or tabular structures. Most graphite crystals are strongly deformed due to dislocations and marked differences in hardness of the enclosing minerals (Kwiecińska, 1980; Taylor et al., 1998). Lath-acicular-feathery structures showing evidence of distortion of crystals (Fig. 4), platy forms with rounded outlines (Fig. 5B), nodule-shaped concentrations, spherulitic aggregates, and palm-shaped and vermicular forms are commonly visible. Unusual forms of graphite, especially pseudodipyramidal, prismatic and tabular crystals showing spiral-layer growth are described by Kvasnitsa et al. (1999).

Mono and polycrystalline aggregates of graphite display very strong anisotropy. Graphite is an optically uniaxial mineral of a negative reflectance sign: $R_{ordinary} > R_{extraordinary}$ (Galopin and Henry, 1972). Graphite shows strong bireflectance and pleochroism, with the intensity depending on the section orientation. Sections parallel to the natural cleavage surfaces are the most readily available in graphite crystals (a–b

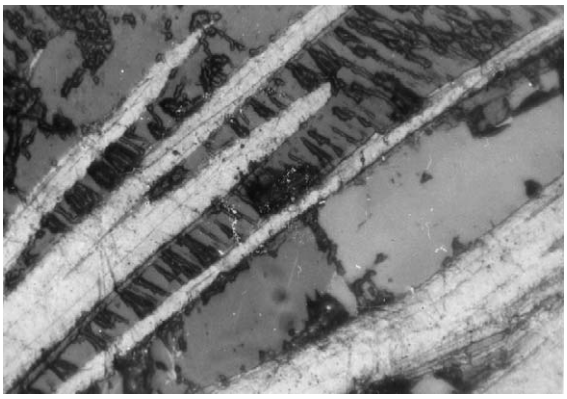

Fig. 10. Graphite with lath-like structure in pyroxene granulite, Sri Lanka. Polished block, reflected light, oil immersion, 1 nicol.

directions), and since they are simultaneously the (001) planes, reflectance measurements are usually made on them (Fig. 8). Cleavage surfaces which are inclined to the basal surface and which could yield data on the optical properties towards *c*-axis are scarce (Palache, 1941). The (001) planes are optically isotropic, whereas reflectance from the planes inclined to the basal pinacoid depends on the direction of polarisation (hence maximum and minimum values).

Reflectance values measured on polished surface blocks show marked differences depending on the degree of graphitization of the organic matter. Bireflectance, however, is always extremely high (Ramdohr, 1980). $R_{o,max}$ reaches 14.40%. $R_{o,min}$ is only 0.5% in graphites from granulite facies rocks (Kwiecińska, 1980). The $\%R_{o,max}$ value is considerably lower than that for natural cleavage surfaces (peels parallel to the basal pinacoid (001)). For $\lambda = 546$ nm, $R_{o,max}$ can range from 17.86% (Kwiecińska et al., 1977) to 18.8% (Koch and Günther, 1995) when measured on graphite samples derived from the amphibolite and granulite facies. Reflectances measured on polished blocks of graphite disseminated in rocks are not comparable with those obtained directly from natural cleavage surfaces, where the reflectance is approximately 20% higher. The way of producing a polished graphite surface of high specular quality is a major problem in reflectance measurements and thus determines the accuracy of the results.

2.5. Derivation

Graphite can be (i) syngenetic, formed through the metamorphic evolution of carbonaceous matter dispersed in the sediments or (ii) epigenetic, originating from precipitation of solid carbon from carbon-saturated C–O–H fluids (Pasteris and Wopenka, 1991; Wopenka and Pasteris, 1993; Rodas et al., 2000). Fully ordered, pure graphite occurring at the highest metamorphic grades is regarded as the final product of the so-called ''graphitization''. Natural graphitization appears to be a continuous, progressive process. The transformation of carbonaceous matter involves structural and compositional changes (Grew, 1974; Diessel and Offler, 1975). The majority of graphite occurrences in the world falls within this category. Graphites have been documented at many sites ranging from upper greenschist–lower amphibolite facies up to granulite facies. The graphite has a biogenic origin, formed from various organic substances, such as aquatic and land plants, kerogen, bituminous matter, and other organic remnants. The identified fragments of organic structures embedded in limestones, phyllites, slates, schists, meta-anthracites, and semi-graphites prove irrefutable evidence of biogenic genesis (Hamilton et al., 1970; Landis, 1971; Carraro and Charrier, 1972; Sedlak, 1973; Diessel and Offler, 1975; Stadler et al., 1976; Diessel et al., 1978; Kwiecińska, 1980; Stach et al., 1982; Barrenechea et al., 1992; Taylor et al., 1998). Graphite occurring in nature is mainly formed under conditions of thermal or regional metamorphism. However, besides the temperature, graphitization of carbonaceous material also requires the input of shear strain and strain energy. The effects of pressure and shear promote molecular ordering of basic structural units in graphite and facilitate preferential alignment of aromatic lamellae and pore coalescence (Bonijoly et al., 1982; Buseck and Huang Bo-Jun, 1985; Wilks et al., 1993; Bustin et al., 1994).

Graphite appearing as scarce impregnations in igneous rocks can also owe its origin to organic matter taken in by the magma in the process of palingenesis.

Physical conditions for graphitization are estimated by several authors in different manner, i.e. Landis (1971) determined graphitization to begin at a temperature of at least 300 °C with fully ordered graphite appearing not before 450 °C and pressure between 2×10^8 Pa (2 kbar) and 6×10^8 Pa (6 kbar). Grew (1974) obtained data of 300–500 °C and over 3×10^8 Pa (3 kbar), respectively. According to Diessel and Offler (1975), graphitization begins within the chlorite zone of the greenschist facies and is completed before the beginning of the amphibolite facies at temperatures from 380 to ~ 450 °C and pressures between 2×10^8 Pa (2 kbar) and 3×10^8 Pa (3 kbar). Kwiecińska (1980) showed perfect, three-dimensional lattice-ordered graphite from the amphibolite and granulite facies.

Well-formed graphite crystals (ca. 1 mm in size) showing tabular hexagonal morphology exist in calcite in Crestmore, Riverside County (California), and also in calcite marble in Pargas (Finland), but with a different shape than the former (rosettes, tiny spheres showing radial interior texture). Natural occurrences of spherical graphite in marbles, pegmatites and

igneous rocks are found in a relatively large number in a region extending from New Jersey through New York and on into Ontario, Canada (Jaszczak, 1995) (Fig. 11).

Considering the inorganic (abiotic) hypothesis of graphite formation, CO and CO_2 play an essential role. Of the reactions proceeding the natural conditions, the most probable are:

$$2CO \rightarrow C + CO_2$$

$$2CO + 2H_2O \rightarrow 2CO_2 + 2H_2$$

$$CO_2 + 2H_2 \rightarrow C + 2H_2O$$

The source of graphite can be:

a) gaseous emanations;
b) reactions of the type: $CaCO_3 + 4H_2 \rightarrow CH_4 + H_2O + Ca(OH)_2$;
c) pyrolitic dissociation of methane: $CH_4 \rightarrow C + 2H_2$ (Salotti et al., 1971);
d) $CH_4 + 4Fe^{3+} = C + 4Fe^{2+} + 4H$ (Ridge, 1976);
e) CO_2 released by the process of silification of limestones during contact metamorphism: $3CaCO_3 + 3SiO_2 \rightarrow Ca_3(Si_3O_9) + 3CO_2$;
f) $6FeCO_3 \rightarrow 2Fe_3O_4 + 5CO_2 + C$ (French and Rosenberg, 1965).

Fig. 11. Spherical graphite. Gooderham, Ontario Canada. Diameter ca. 5 mm. Photo courtesy of Dr John Jaszczak, Michigan Technical University, USA.

Marx (1971), based on the studies of graphite specimens, introduced the electrochemical theory of graphite formation in which the parageneses pyrrhotite-, magnetite-, and siderite-graphite exist. Similar genesis of graphite from magnetite rocks of Krzemianka (Poland) is described by Kucha et al. (1979).

In general, precipitation of graphite from carbon-bearing fluids includes: isobaric cooling or isothermal pressure increase, hydration reactions, fugacity of oxygen changes (fO_2), and mixing of different C–O–H fluids. The source for that fluids could be magmatic (Kvasnitsa et al., 1999), mantle-derived fluids, metamorphic decarbonation reactions, and devolatilization of organic matter (Rodas et al., 2000). Also catalytic graphitization and thermal dissociation of methane have to be considered.

Well-ordered graphite particles are also found in meteorites (Jaszczak, 1995). In the Allende meteorite (type of carbonaceous chondrite) graphite is similar in size and appearance to the fullerene-related structures: carbon onions and nanotubes (Becker et al., 1993). From the Murchison meteorite, spherical graphite particles, up to several microns across, have been isolated and described as being of interstellar origin. The interstellar spherical graphite particles have a concentric layered internal structure as revealed by TEM investigations. Spherulitic graphite, known as cliftonite, occurs with diameters ranging from 10 μm to 1 mm in some iron meteorites (Brett and Higgins, 1969). Micron-sized spherical graphites, formed from the vapor phase, occur in natural coke from the St. Ingbert mine, Saar Basin (Germany), in the La Rasa mine (Spain), and in the Lower Silesia Coal Basin (Poland) (Stach, 1951; Kwiecińska, 1967; Kwiecińska et al., 1995).

Publications dealing with synthetic graphitization demonstrate, for example, the process of formation of liquid crystals, the so-called mesophase (Brooks and Taylor, 1965; Marsh, 1973).

2.6. Practical importance

Natural graphite is used in a variety of applications such as lubricants, seals, insulation, fillers, refractories, electrodes, and moderators in nuclear reactors. Specific properties of graphite result in its increasing importance in the refractory industry (Galos and Wyszomirski, 2001). Natural graphites

are used for the production of a wide range of modern refractories, such as magnesia-graphite or alumina-graphite products. A larger size of graphite crystallites in natural graphite grades, compared to synthetic ones, results in their higher resistance to oxidation. This feature, i.e. relatively high resistance to oxidation, is observed especially in the case of natural flake graphite grades.

3. Semi-graphite

3.1. Origin of term

The term has been used to describe the transitional phase in the stage of coalification–graphitization of carbonaceous matter occurring in sediments with a high content of graphitic carbon.

Synonyms and analogous terms:

Graphocite—Schopf (1966)
Poorly ordered graphite—Křibek et al. (1994)

3.2. Definition

The natural precursors of semi-graphite are anthracite and meta-anthracite when they are subjected to a high geothermal gradient, and/or to high pressure and/or tectonic stress.

Comment. To recognise semi-graphite and distinguish it from graphite particles, especially when they are dispersed in graphitised sediments, is not easy under reflected light microscopy. Both of them have similar optical properties (structure, anisotropy, etc.). The differentiation of pure graphite and semi-graphite is mainly based on X-ray analysis (Kwiecińska, 1978), transmission electron microscopy (TEM) investigations (McCartney and Ergun, 1965; Kwiecińska and Nowak, 1997), measurements of maximum reflectance (%$R_{o,max}$) (Kwiecińska, 1980), and determination of H/C atomic ratios (see Section 2). Analysis of structural parameters (interlayer spacing d (002), the crystallite diameter La [measured in the carbon layer planes], and the height Lc [measured perpendicular to the carbon layers]) shows a substantial increase from anthracite and meta-anthracite to semi-graphite. La rises up to 2500 Å and Lc takes values about 500 Å. The interlayer spacing (d_{002}) is between 3.38 and 3.37 Å. There is a visible progressive ordering of the molecular structure in comparison with anthracites and meta-anthracites. The number and intensity of the hkl reflections increases in semi-graphites.

The beginning of pre-graphitization, based on maximum reflectance measurements, could be at $R_{o,max}$ = 6–6.5%, corresponding to 95% C. The stage of semi-graphite is reached at a $R_{o,max}$ of up to 9% and $R_{o,min}$ = 2% (Kwiecińska, 1980; Taylor et al., 1998).

The exact identification of semi-graphite requires additional studies under TEM. TEM investigations can reveal differences between the habit, shape, and size of individual particles which belong to graphitic or semi-graphitic domains (Kwiecińska, 1967, 1980; Hamilton et al., 1970; Landis, 1971). By the application of selected-area electron diffraction (SAD), the presence of graphitic or semi-graphitic phases can also be detected (McCartney and Ergun, 1965; Bonijoly et al., 1982; Deurbergue et al., 1987; Kwiecińska and Nowak, 1997). Recently high-resolution transmission electron microscopy (HRTEM) has thrown new light on the ultrafine structure of carbonaceous matter (Wopenka and Pasteris, 1993; Taylor et al., 1998). At the semi-graphite stage, extensive coalescence of pores is visible. The number of aromatic layers in the stacks increases from 2–3 to more than 40. During the same phase, layers rapidly become more rigid and planar. The turbostratic structure disappears and a partial graphitization takes place. According to Oberlin and Terriere (1975) and Rouzaud and Oberlin (1983), semi-graphitization requires not only high temperatures but also high pressures enhanced by shearing and stretching. Diessel et al. (1978) also concluded that high pressure accelerates graphitization.

In the same specimen, which often represents heterogeneous material, three phases may coexist (intermixed) (Kwiecińska and Nowak, 1997):

1. anthracites which are microporous and have two-dimensional (turbostratic) crystalline order;
2. semi-graphites which are partially graphitized and macroporous;
3. pure graphites which usually consist of small disks or hexagonal shaped lamellae.

For an exact examination of such particles, X-ray data are not sufficient because they yield an average

value and do not represent the crystallinity of each particle (Deurbergue et al., 1987). Only selected-area electron diffraction (SAD) is able to distinguish between the two- and three-dimensional crystalline order of single particles. The rank stage of semi-graphite commonly corresponds to low-grade metamorphism of rocks (Taylor et al., 1998). According to McCartney and Ergun (1965) and Diessel et al. (1978), semi-graphite quite often occurs at the stage of meta-anthracite where it is associated with organic particles. Křibek et al. (1994) also revealed the coexistence of various types of graphitized particles derived from different types of carbonaceous matter, such as amorphous kerogen, bitumens, and graptolites; and from a gaseous phase as a product of epitaxial growth of carbon. They concluded that the differences in the degree of graphitization of the organic substance in low-grade metamorphosed rocks can be mainly related to the initial nature of the components and to their premetamorphic history.

4. Natural coke

4.1. Origin of the term

The term natural coke has been used to describe coal thermally affected by an igneous intrusive body. The term was introduced by Hoehne (1941).

Synonyms and analogous terms:

Geological coke
Burnt coke
Cinder
Jhama
Thermally metamorphosed coal (Taylor et al., 1998)

4.2. Definition

Natural coke is coal altered by the relatively local elevated heat flow caused by an intrusive body.

Comment. The kind of coal alteration depends on the temperature of the intrusion, the duration of magmatic heating and the distance from direct contact with the igneous rock. The influence of thermal metamorphism on coal is very differentiated. The width of the contact zone is usually small, up to several centimetres (Kwiecińska, 1967; Jones and Creaney, 1977; Kwiecińska et al., 1992, 1995), but sometimes much greater, even up to kilometres in width (Taylor et al., 1998). Hence, the thermal influence depends on the thickness, nature and form of the intrusive body as well as the composition and rank of the intruded organic-rich rock (Marshall, 1945).

4.3. Physical properties

4.3.1. Macroscopic observations

Natural coke is usually dull, compact and hard. It has vacuoles (pores) which are empty or infilled with mineral matter, especially calcite. The textural features such as the size, shape, distribution and orientation of pores are variable (Stach, 1952). The immediate contact between the igneous intrusive body and the coal may be sharp and planar or it may be diffuse and irregular (Taylor et al., 1998).

Microscopic observations. The optical changes of the coal induced by the thermal metamorphism depend on the initial rank of the coal and the level of maturity at the time of intrusion. These are the most important factors. In natural coke formed from bituminous coals three groups of microconstituents may be recognized:

1. matrix (groundmass) formed by total alteration of vitrinite and liptinite;
2. macerals of the inertinite group with preserved structures and textures visible in the unaltered coal;
3. new components, which are partly high-carbon material and partly mineral matter, formed due to the intrusion (Taylor et al., 1998).

Entirely coked vitrinite, especially from bituminous coals, often exhibits mosaic structure (fine, medium, coarse) showing variable degree of optical anisotropy. The anisotropy and reflectance increase with the temperature of alteration. The occurrence of mosaic structure is one of the primary features which distinguish natural coke from natural char (see Section 5).

Fracture analysis of natural coke observed with scanning electron microscopy (SEM) reveals detailed information on its texture. The following main coke types can be recognised: pores (Fig. 12), spheres (hollow and solid) (Fig. 13), folds (Fig. 14), and holes

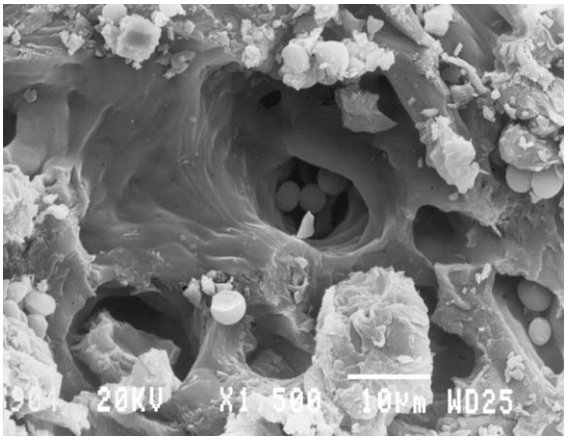

Fig. 12. Visible pores. La Rasa mine. Tineo, Asturias, Spain. Scanning electron microscopy.

(Figs. 15 and 16) (Kwiecińska et al., 1992, 1995; Vleeskens et al., 1994; Kwiecińska and Nowak, 1997). In microscopic profiles taken perpendicular to intrusions, we can observe transitional zones containing shattered, contorted, mylonitized coal, and, finally, in considerable distance from the intrusion, undistorted, laminated coal. Inertinite macerals in general exhibit little morphological change during thermal (contact) metamorphism, but they show significant increase in reflectance.

Among the new organic components formed during the intrusion, we can distinguish carbona-

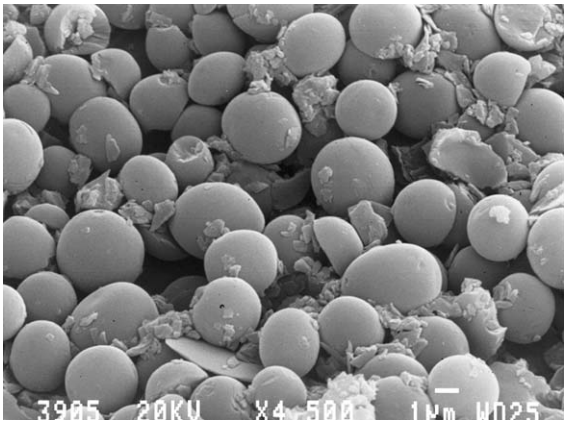

Fig. 13. Solid spheres. La Rasa mine. Tineo, Asturias, Spain. Scanning electron microscopy.

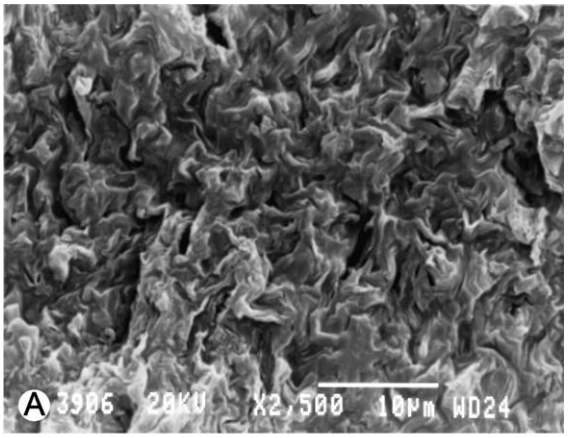

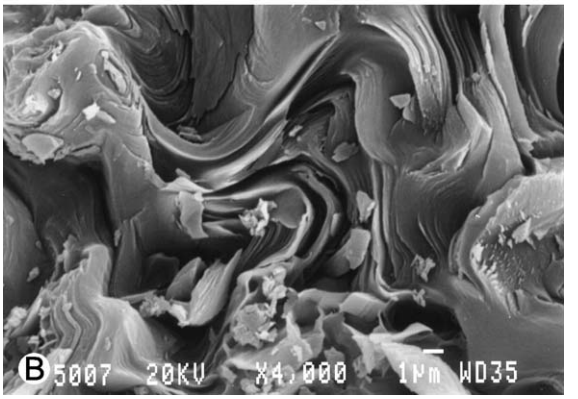

Fig. 14. (A) Folds formed during plasticity. La Rasa mine. Tineo, Asturias, Spain. Scanning electron microscopy; (B) Folds formed during plasticity. La Rasa mine. Tineo, Asturias, Spain. Scanning electron microscopy.

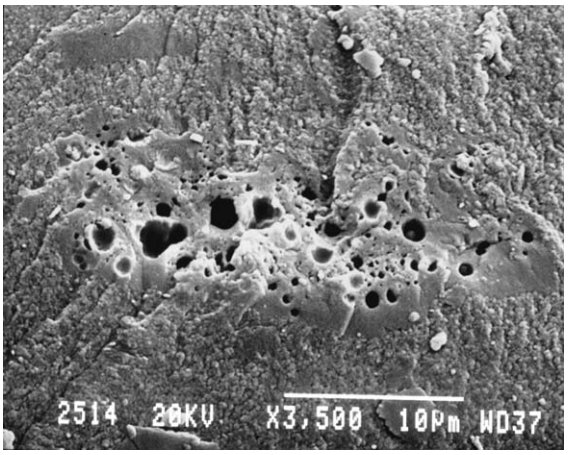

Fig. 15. Small devolatilization holes. Wałbrzych mine, The Lower Silesian Coal Basin, Poland. Scanning electron microscopy.

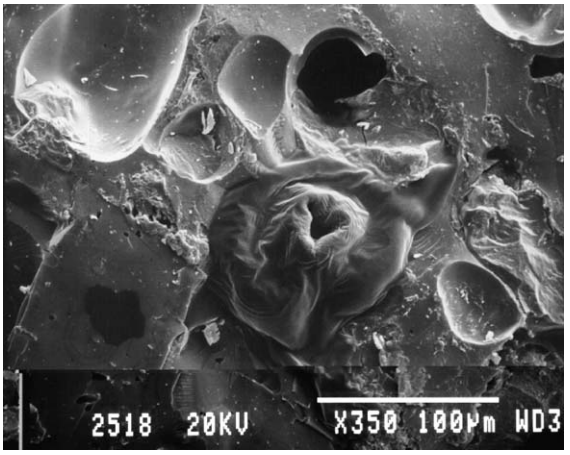

Fig. 16. Locally strongly developed plasticity features. Wałbrzych mine, The Lower Silesian Coal Basin, Poland. Scanning electron microscopy.

ceous material deposited from a gas phase formed by the chemical cracking of volatile matter (Goodarzi et al., 1992). This organic matter occurs as small spheres, 2–5 μm in diameter, infilling vesicles within thermally metamorphosed carbonaceous rocks (Marsh, 1973) or as pyrolytic carbon (Goodarzi, 1985) which can appear in layers, lining or filling cavities. Such solid spheres are so-called "pyrocarbons" (Kwiecińska et al., 1995) and are evidence for increased molecular ordering approaching graphitization. This is mesophase material consisting of semi-graphitic and graphitic spheroliths with concentric structure formed by deposition from the gaseous phase.

Minerals occurring in natural cokes are little changed. Mainly pyrite (FeS_2) changes to FeS or Fe_2O_3. The crystal shape of minerals is the evidence of hydrothermal activity in the contact zone. The temperature attained in the aureole can be assessed from mineralogical observations (Ward et al., 1989). Sometimes pyrite is used as a geological thermometer, showing incidental hot spots in contact with the dyke (Kwiecińska et al., 1992).

The reflectance of vitrinite in natural cokes has been found to be related to various other physical and chemical characteristics (Taylor et al., 1998). The maximum reflectance value can reach up to 11%$R_{o,max}$ in the coked, thermally, altered coal (Teichmüller, 1973). A reflectance discontinuity occurs at the boundary between the two quite different kinds of material (vitrinite and mesophase or coke) in areas where vitrinite has been converted to mesophase or coke (Taylor et al., 1998).

5. Natural char

5.1. Origin of term

The term natural char was proposed by Petersen (1998) to describe organic particles with pyrolysis char morphology in coal seams and carbonaceous mudstones.

5.2. Definition

Natural char has a higher reflectance than the associated huminite/vitrinite, and commonly the reflectance is also higher than the associated inertinite. Natural char is characterised by a random distribution of pores and a varying porosity.

Comment. Due to the morphology of natural char, it cannot be grouped together with one of the established inertinite group macerals (ICCP, 2001). However, the morphological similarity to chars derived from low-temperature pyrolysation of coal enables classification of the natural char by using a combustion char classification system, for example the systems published by Bailey et al. (1990) or Rosenberg et al. (1996), or the system used by the ICCP Combustion Working Group.

5.3. Occurrence

Natural char seems to occur in coals and carbonaceous mudstones from all over the world, independent of the geological age of the deposits. Natural char has been detected in coals and coaly deposits from the Carboniferous in USA, the Permian in Australia, the Middle Jurassic from North-East Greenland (Kuhn Ø) and the Danish North Sea, the Upper Jurassic from North-East Greenland (Wollaston Forland), the Cretaceous from West Greenland, and the Tertiary from Colombia. The rank of the deposits ranges from lignite/sub-bituminous to medium volatile bituminous (random vitrinite reflectance range: app. 0.35–0.5%R_o to app. 1.2%R_o). Natural char is volumetri-

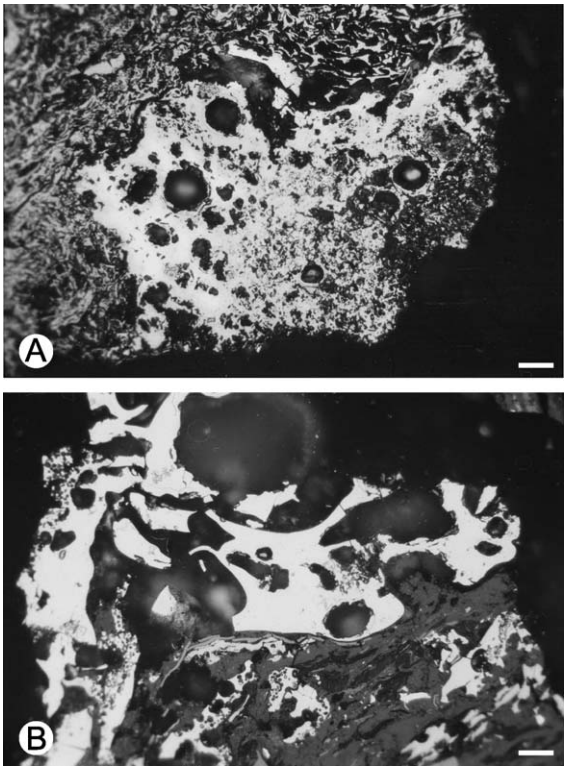

Fig. 17. Natural char with mixed dense/porous char morphology. (A) Middle Jurassic coal of sub-bituminous A rank, Bastians Dal, North-East Greenland; (B) Permian Drayton coal of high vol. bituminous B rank, Australia. Reflected light microscopy, oil immersion. Scale ~ 30 μm.

cally of minor importance as it in general amounts to < 1 vol.%, but up to 3 vol.% has been measured in carbonaceous mudstones from North-East Greenland. In general, the inertinite content of the deposits is high, from 14 to 61 vol.%, and mainly it is above 30 vol.%.

5.4. Physical properties

Microscopically natural char is characterised by randomly distributed pores and varying porosity, shape, and size (Figs. 17–19). A faint concentric ordering/layering of the organic matter around the pores may be present. The colour in reflected white light is light grey to white, and the reflectance is always higher than the associated huminite/vitrinite. Reflectance measurements (random) on char particles in low-rank ($R_{o,vitrinite}$ ~ 0.50%) Middle Jurassic coal samples from Bastians Dal, Kuhn Ø, North–East Greenland, yield reflectance values between 2.26%$R_{o,char}$ and 5.43%$R_{o,char}$, but with the majority of the reflectance values being above 4%$R_{o,char}$ (Table 2).

The most common morphologies of natural char are dense irregular morphotypes corresponding to the combustion char morphotypes 'mixed dense/porous' (Fig. 17), 'inertoid' and 'solid' (Fig. 18), but porous spherical types corresponding to the combustion char morphotypes 'tenuisphere' and 'crassisphere' also occur (Fig. 19) (Petersen, 1998). The size of natural char varies from approximately 30 to up to 900 μm (Petersen, 1998; Petersen et al., 2000).

The macerals most likely to be confused with natural char are fusinite (charcoal), semifusinite and funginite; but the random pore distribution in natural char is the primary criterion that distinguishes it from these three inertinite macerals. In contrast to natural char, fusinite (charcoal), which is formed by burning of fresh and more or less unaltered plant tissues, often has a well-preserved cellular structure with rays of cells and thin cell walls (Cope and

Table 2
Reflectance values of natural char in low-rank coals from Bastians Dal, Kuhn Ø, North-East Greenland

Sample	Particle no.	%$R_{o,char}$
878	particle 1	5.19
	particle 2	4.17
		4.05
	particle 3	3.56
	particle 4	5.41
		5.43
	particle 5	5.05
	particle 6	5.16
		5.09
		5.34
		5.30
	particle 7	5.39
884	particle 1	4.18
		3.95
		4.38
		4.63
		3.87
		4.11
887	particle 1	5.22
		5.26
896	particle 1	2.27
		2.28

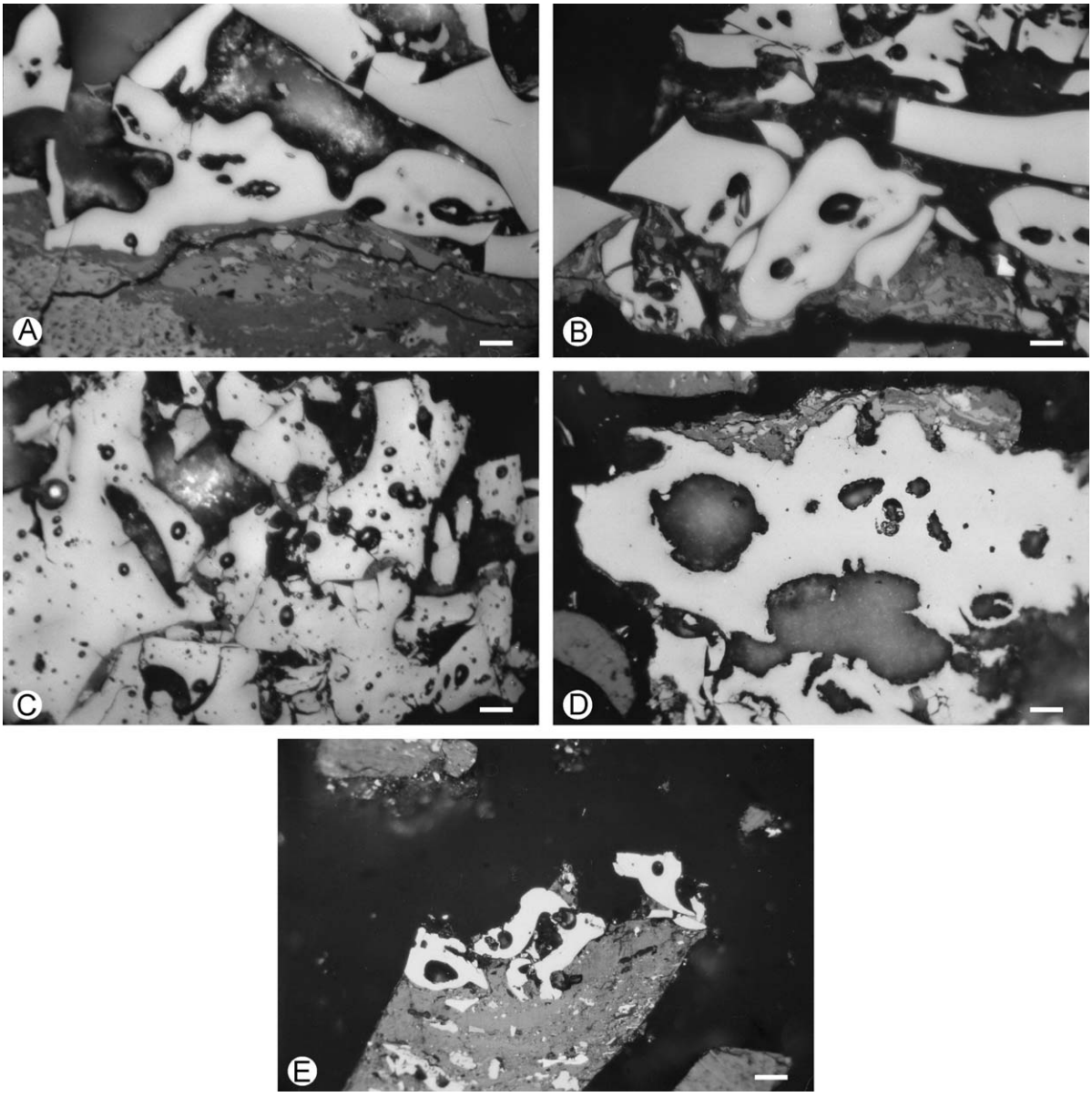

Fig. 18. Natural char with inertoid and solid char morphology. (A–C) Middle Jurassic coal (seam T2) of high vol. bituminous A rank in the 3/7–4 well, Norwegian North Sea; (D) Middle Jurassic coal (seam X) of high vol. bituminous A rank in the Lulita-1X well, Danish North Sea; (E) Tertiary Cerrejon coal of high vol. bituminous C rank, Colombia. Reflected light microscopy, oil immersion. Scale ~ 30 μm.

Chaloner, 1985; Scott, 1989, 2000; Taylor et al., 1998; ICCP, 2001). Semifusinite has a similar morphology, but the cell walls are thicker (swollen) and the cell cavities are only partly visible and of varying size and shape. Funginite consists of fungal remains (spores, sclerotia, hyphae), and the maceral is mainly roundish to oval and contains one or more chambers showing a regular pattern (Stach and Pickhardt, 1964; Taylor et al., 1998; Lyons, 2000; ICCP, 2001).

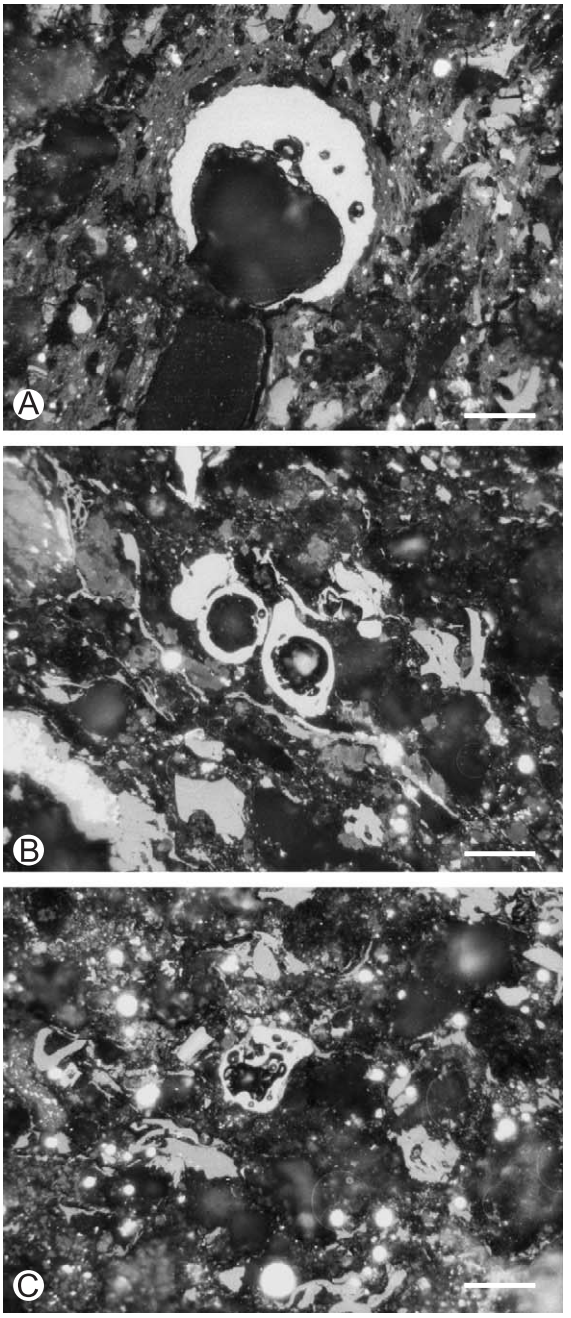

Fig. 19. Natural char with porous spherical char morphology. (A) Middle Jurassic coal of sub-bituminous A rank, Bastians Dal, North-East Greenland; (B–C) Cretaceous sediments of low vol. bituminous rank in the Gro-3 well, West Greenland. Reflected light microscopy, oil immersion. Scale ~ 30 μm.

In contrast to natural coke with mosaic structure (see Section 4), which typically is the dominant coke type in natural coke formed from bituminous coals at temperatures above 500 °C, mosaic structure has not been observed in natural chars.

5.5. Derivation

Natural char is formed by the influence of heat from fire on (1) coal or (2) gelified organic matter in a peat. The complex and varying morphology of the particles is related to degassing of volatiles from the coalified or humified organic matter. The faint concentric ordering of the organic matter around the pores is a feature that is well-known from degassing pores in laboratory-derived low-temperature chars and indicates that the organic matter was in a plastic phase during heating. The observed morphology of natural char is characteristic of chars derived from experimental pyrolysation of coal, in particular low-temperature chars derived, for example, from a muffle furnace where the maximum temperature does not exceed 900 °C (Petersen, 1998). This suggests that the formation of natural char occurs at relatively low temperatures. Generally, the low heating rates and low final temperatures form denser char morphotypes. In contrast, pulverised fuel combustion chars formed at much higher temperatures generally have significantly higher porosity.

'Local' char formation from different macerals in coal has been shown experimentally by pyrolysis of coal under conditions of slow heating rate (Unsworth et al., 1991). This suggests that natural char formation can occur by heat affection of coal, and may also explain the co-occurrence of natural char and unaltered coal. However, where the formation of the inertinite and natural char was simultaneous during burning (wildfire), the natural char may be an additional palaeoenvironmental indicator of peat fire. The reflectance of inertinite can be related to the burning-temperature during formation of the inertinite (Jones et al., 1991; Scott and Jones, 1994), and reflectance measurements on inertinite intimately associated with natural char in inertinite-rich mudstones, North-East Greenland, yielded burning temperatures of 400–700 °C (Bojesen-Koefoed et al., 1997). This would be consistent with a ground fire or surface fire, where burning of gelified organic matter may have occurred.

Acknowledgements

The work by B. Kwiecińska was supported by the AGH University of Science and Technology, Krakow (research project no. 11.11.140.408), and the work by H.I. Petersen by the Geological Survey of Denmark and Greenland (GEUS), Copenhagen.

References

Bailey, J.G., Tate, A., Diessel, C.F.K., Wall, T.F., 1990. A char morphology system with applications to coal combustion. Fuel 69, 225–239.

Barrenechea, J.F., Rodas, M., Arche, A., 1992. Relation between graphitization of organic matter and clay mineralogy, Silurian black shales in central Spain. Mineral. Mag. 56, 477–485.

Becker, L., McDonald, G.D., Bada, J.L., 1993. Carbon onions in meteorites. Nature 361, 595.

Bernal, J.D., 1924. The structure of graphite. Proc. R. Soc. A106, 749–773.

Bojesen-Koefoed, J.A., Petersen, H.I., Surlyk, F., Vosgerau, H., 1997. Organic petrography and geochemistry of inertinite-rich mudstones, Jakobsstigen Formation, Upper Jurassic, northeast Greenland: indications of forest fires and variations in relative sea-level. Int. J. Coal Geol. 34, 345–370.

Bonijoly, M., Oberlin, M., Oberlin, A., 1982. A possible mechanism for natural graphite formation. Int. J. Coal Geol. 1, 283–312.

Brett, R., Higgins, G.T., 1969. Cliftonite: a proposed origin, and it is bearing on the origin of diamonds in meteorites. Geochim. Cosmochim. Acta 33, 1473–1476.

Brooks, J.D., Taylor, G.H., 1965. The formation of graphitizing carbons from liquid phase. Carbon 3, 185–193.

Buseck, P.R., Huang Bo-Jun, 1985. Conversion of carbonaceous material to graphite during metamorphism. Geochim. Cosmochim. Acta 49, 2003–2016.

Bustin, R.M., Ross, J.V., Rouzaud, J.N., 1994. Experimental evidence for the mechanisms of graphite formation from an anthracite—a STEM investigation. Proc. Int. Symp. Coal and Org. Petrol., Fukuoka.

Carraro, F., Charrier, G., 1972. Paleontological evidence for the late Carboniferous age of the volcano detrital cover of the "micascisti eclogitici" (Sesia-Lanzo Zone Western Alps). Boll. Soc. Geol. Ital. 91, 185–194.

Cope, M.J., Chaloner, W.G., 1985. Wildfire: an interaction of biological and physical processes. In: Tiffney, B.H. (Ed.), Geological Factors and the Evolution of Plants. Yale University Press, New Haven, pp. 257–277.

Deurbergue, A., Oberlin, A., Oh, J.H., Rouzaud, J.N., 1987. Graphitization of Korean anthracites as studied by transmission electron microscopy and X-ray diffraction. Int. J. Coal Geol. 9, 375–393.

Diessel, C.F.K., Offler, R., 1975. Change in physical properties of coalified and graphitized phytoclasts with grade of metamorphism. Neues Jahrb. Mineral., Monatsh. H. 1, 11–26.

Diessel, C.F.K., Brothers, R.N., Black, P.M., 1978. Coalification and graphitization in high-pressure schists in New Caledonia. Contrib. Mineral. Petrol. 68, 63–78.

French, B.M., Rosenberg, P.E., 1965. Siderite ($FeCO_3$): thermal decomposition in equilibrium with graphite. Science 147, 1283–1284.

Galopin, R., Henry, N.F.M., 1972. Microscopic Study of Opaque Minerals. Heffer, Cambridge. 322 pp.

Galos, K., Wyszomirski, P., 2001. Some refracting raw materials—mineralogical and technological characteristics. Ceram.-Pol. Ceram. Bull. 64, 59–68 (in Polish).

Goodarzi, F., 1985. Characteristics of pyrolytic carbon in Canadian coals. Fuel 64, 1672–1676.

Goodarzi, F., Eckstrand, O.R., Snowdon, L., Williamson, B., Stasiuk, L.D., 1992. Thermal metamorphism of bitumen in Archean rocks by ultramafic volcanic flows. Int. J. Coal Geol. 20, 165–178.

Grew, E.S., 1974. Carbonaceous material in some metamorphic rocks of New England and other areas. J. Geol. 82, 50–73.

Hamilton, L.H., Ramsden, A.R., Stephens, J.F., 1970. Fossiliferous graphite from Undercliff, New South Wales. J. Geol. Soc. Aust. 17, 31–37.

Hoehne, K., 1941. Über die Kontaktwirkung von Porphyr auf Steinkohle Flöze und die hydrothermalen Gangtruemer im Waldenburger Bergbaugebiet. Jahrb. Reichsstelle Bodenforsch. 62, 438–498.

Hull, A.W., 1917. A new method of X-ray crystal analysis. Phys. Rev. 10, 661–696.

International Committee for Coal and Organic Petrology, 1998. The new vitrinite classification (ICCP System 1994). Fuel 77, 349–358.

International Committee for Coal and Organic Petrology, 2001. The new inertinite classification (ICCP System 1994). Fuel 80, 459–471.

Jaszczak, J.A., 1994. Famous graphite crystals from Sterling Hill, New Jersey. Pickling Table 35, 6–11.

Jaszczak, J.A., 1995. Graphite: flat, fibrous and spherical. In: Mendenhall, G.D. (Ed.), Mesomolecules from Molecules to Materials. Chapman & Hall, London, pp. 161–180.

Jones, J.M., Creaney, S., 1977. Optical character of thermally metamorphosed coals of northern England. J. Microsc. 109 (pt. 1), 105–118.

Jones, T.P., Scott, A.C., Cope, M., 1991. Reflectance measurements and the temperature of formation of modern charcoals and implications for studies of fusain. Bull. Soc. Fr. 162, 193–200.

Koch, J., Günther, M., 1995. Relationship between random and maximum vitrinite reflectance. Fuel 74, 1687–1691.

Křibek, B., Hrabal, J., Landais, P., Hladikova, J., 1994. The association of poorly ordered graphite, coke and bitumens in greenschist facies rocks of the ponikla group, Lugicum, Czech Republic: the result of graphitization of various types of carbonaceous matter. J. Metamorph. Geol. 12, 493–503.

Kucha, H., Kwiecińska, B., Piestrzyński, A., Wieczorek, A., 1979. On the genesis of graphite from magnetite rocks of Krzemianka (NE Poland). Mineral. Pol. 10, 81–88.

Kvasnitsa, V., Yatsenko, V.G., Jaszczak, J.A., 1999. Disclinations in unusual graphite from anorthosites of Ukraine. Can. Mineral. 37, 951–960.

Kwiecińska, B., 1967. Coked coals from the Walbrzych. Prace Mineralogiczne, vol. 9. PAN, Kraków, pp. 1–81. In Polish.

Kwiecińska, B., 1978. On the rhombohedral modification in natural graphites and semigraphites. Mineral. Pol. 95, 3–15.

Kwiecińska, B., 1980. Mineralogy of natural graphites. Prace Mineralogiczne, vol. 67. PAN, Kraków, pp. 1–87.

Kwiecińska, B., Nowak, G., 1997. Highly metamorphosed coals from the Lower Silesian Coal Basin (SW Poland). Proc. XIII Int. Congr. Carboniferous and Permian, Kraków, Prace PIG, vol. CLVII. Polish Geological Institute, Warsaw, pp. 247–255.

Kwiecińska, B., Murchison, D.G., Scott, E., 1977. Optical properties of graphite. J. Microsc. 109, 289–302.

Kwiecińska, B., Hamburg, G., Vleeskens, J., 1992. Formation temperatures of natural coke in the Lower Silesian Coal Basin, Poland. Evidence from pyrite and clays by SEM–EDX. Int. J. Coal Geol. 21, 217–235.

Kwiecińska, B., Muszyński, M., Vleeskens, J., Hamburg, G., 1995. Natural coke from the La Rasa mine, Tineo, Spain. Mineral. Pol. 26, 3–14.

Landis, C.A., 1971. Graphitization of dispersed carbonaceous material in metamorphic rocks. Contrib. Mineral. Petrol. 30, 34–45.

Lyons, P.C., 2000. Funginite and secretinite—two new macerals of the inertinite maceral group. Int. J. Coal Geol. 44, 95–98.

Marsh, H., 1973. Structural analysis of cokes, carbons and graphites by phase-contrast electron microscopy. Northern Coke Research Com. Progress. Report 94.

Marshall, C.E., 1945. Petrology of natural coke. Fuel 24, 120–126.

Marx, P.C., 1971. On the electrochemical origin of natural graphite. Am. Mineral. 56, 336–338.

McCartney, J.F., Ergun, S., 1965. Electron microscopy of graphite crystallites in meta-anthracite. Nature 205, 962–964.

Oberlin, A., Terriere, G., 1975. Graphitization studies of anthracites by high-resolution electron microscopy. Carbon 13, 367–376.

Palache, C., 1941. Contributions to the mineralogy of Sterling Hill, New Jersey: morphology of graphite, arsenopyrite, pyrite and arsenic. Am. Mineral. 26, 709–717.

Pasteris, J.D., Wopenka, B., 1991. Raman spectra of graphite as indicators of degree of metamorphism. Can. Mineral. 29, 1–9.

Petersen, H.I., 1998. Morphology, formation and palaeo-environmental implications of naturally formed char particles in coals and carbonaceous mudstones. Fuel 77, 1177–1183.

Petersen, H.I., Andsbjerg, J., Bojesen-Koefoed, J.A., Nytoft, H.P., 2000. Coal-generated oil: source rock evaluation and petroleum geochemistry of the Lulita oilfield, Danish North Sea. J. Pet. Geol. 23, 55–90.

Ramdohr, P., 1980. The Ore Minerals and their Intergrowth. Pergamon, Oxford, UK.

Reynolds, W.N., 1968. Physical properties of graphite. Mater. Sci. Ser., Elsevier, Amsterdam.

Ridge, J.D., 1976. Annotated Bibliographies of Mineral Deposits in Africa, Asia (exclusive of the USSR) and Australia. The Pennsylvania State University, College of Earth and Mineral Sciences, Pennsylvania.

Rodas, M., Luque, F.J., Barrenechea, J.F., Fernandez-Caliani, J.C., Miras, A., Fernandez-Rodriguez, C., 2000. Graphite occurrences in the low-pressure/high-temperature metamorphic belt of the Sierra de Aracena (southern Iberian Massif). Mineral. Mag. 64, 801–814.

Rosenberg, P., Petersen, H.I., Thomsen, E., 1996. Combustion char morphology related to combustion temperature and coal petrography. Fuel 75, 1071–1082.

Rouzaud, J.N., Oberlin, A., 1983. Contribution of high resolution transmission electron microscopy (TEM) to organic material characterization and interpretation of their reflectance. In: Durand, B. (Ed.), Thermal Phenomena in Sedimentary Basins. Technip, Paris, pp. 127–134.

Salotti, C.A., Heinrich, E.W., Giardini, A.A., 1971. Abiotic carbon and formation of graphite deposits. Econ. Geol. 66, 929–932.

Schopf, J.M., 1966. Definitions of peat and coal and of graphite that terminates the coal series (graphocite). J. Geol. 74, 584–592.

Scott, A., 1989. Observations on the nature and origin of fusain. Int. J. Coal Geol. 12, 443–475.

Scott, A.C., 2000. The Pre-Quaternary history of fire. Palaeogeogr. Palaeoclimatol. Palaeoecol. 164, 281–329.

Scott, A.C., Jones, T.P., 1994. The nature and influence of fire in Carboniferous ecosystems. Palaeogeogr. Palaeoclimatol. Palaeoecol. 106, 91–112.

Sedlak, W., 1973. U źródeł Nowej Nauki (in Polish). Paleobiochemia, Warszawa. 123 pp.

Stach, E., 1951. Ein geologischer Koks im Saarkarbon. Z. Dtsch. Geol. Ges. 103, 233–237.

Stach, E., 1952. Mikroskopie naturlicher Kokse. Handb. Mikrosk. Tech. II, 411–442.

Stach, E., Pickhardt, W., 1964. Tertiäre und karbonische Pilzreste (Sklerotinit). Fortschr. Geol. Rheinl. Westfal. 12, 377–392.

Stach, E., Mackowsky, M.-Th., Teichmüller, M., Taylor, G.H., Chandra, D., Teichmüller, R., 1982. Stach's Textbook of Coal Petrology, 3rd ed. Gebrüder Borntraeger, Berlin-Stuttgart. 535 pp.

Stadler, G., Teichmüller, M., Teichmüller, R., 1976. Zur geothermischen Geschichte des Karbons von Manno bei Lugano und des ''Karbons'' von Falletti (Sesia Zone der Westalpen). Neues Jahrb. Geol. Paläontol. Abh. 152, 177–198.

Taylor, G.H., Teichmüller, M., Davis, A., Diessel, C.F.K., Littke, R., Robert, P., 1998. Organic Petrology. Gebrüder Borntraeger, Berlin-Stuttgart. 704 pp.

Teichmüller, M., 1973. Zur petrographie und Genese von Naturkoksen in Flöz Praesident/Helene der Zeche Friederick Heinrich bei Kamp-Bintfort, linker Niederrhein. Geol. Mitt. Aachen 12, 219–254.

Ubbelohde, A.R., Lewis, F.A., 1960. Graphite and its Crystal Compounds. Oxford University Press, Oxford.

Unsworth, J.F., Barratt, D.J., Roberts, P.T., 1991. Coal quality and combustion performance: Part B. Coal Sci. Technol., vol. 19. Elsevier, Amsterdam. 638 pp.

Vleeskens, J., Kwiecińska, B., Roos, M., Hamburg, G., 1994. Coke forms in nature and in power utilities. Interpretation with SEM. Fuel 73, 816–822.

Ward, C.R., Warbrooke, P.R., Roberts, F.J., 1989. Geochemical and mineralogical changes in a coal seam due to contact metamorphism. Int. J. Coal. Geol. 11, 105–125.

Werner, A.G., 1789. Versuch einer Erklarung der Enstehung der Vulkane durch die Entzundung machtiger Steinkohlenschichten. Zürich.

Wilks, K.R., Mastalerz, M., Bustin, R.M., Ross, J.V., 1993. The effect of experimental deformation on the graphitization of Pennsylvania anthracite. Int. J. Coal Geol. 24, 347–369.

Wopenka, B., Pasteris, J.D., 1993. Structural characterization of kerogens to granulite-facies graphite: applicability of Raman microprobe spectroscopy. Am. Mineral. 78, 533–557.